E6* oncoprotein expression of human papillomavirus type-16 determines different ultraviolet sensitivity related to glutathione and glutathione peroxidase antioxidant defence

Mouret S, Sauvaigo S, Peinnequin A, Favier A, Beani J-C, Leccia M-T. E6* oncoprotein expression of human papillomavirus type-16 determines different ultraviolet sensitivity related to glutathione and glutathione peroxidase antioxidant defence.
Exp Dermatol 2005: 14: 401–410. © Blackwell Munksgaard, 2005

Abstract: Clinical observations of non-melanoma skin cancer in immunocompromised patients, such as organ transplant recipients, suggest co-operative effects of human papillomavirus (HPV) and ultraviolet (UV) radiation. The aim of the present study is to evaluate UV sensitivity and DNA damage formation according to antioxidant status in HPV16-infected keratinocytes. We used SKv cell lines, infected with HPV16 and well characterized for their proliferative and tumorigenic capacities. We showed that SKv cell lines presented various E6* (a truncated form of E6) RNA levels. We demonstrated that the higher oncoprotein RNA expression level was associated with a higher resistance to solar-simulated radiation, more specifically to UVB radiation and to hydrogen peroxide. Moreover, this high resistance was associated with a low oxidative DNA damage formation after UV radiation and was related to high glutathione content and glutathione peroxidase activities. Therefore, the results of our study suggest that E6* levels could modulate the glutathione/glutathione peroxidase pathway providing a mechanism to protect HPV-infected keratinocytes against an environmental oxidative stress, such as UV radiation.

Stéphane Mouret[1], Sylvie Sauvaigo[2], André Peinnequin[3], Alain Favier[2], Jean-Claude Beani[1] and Marie-Thérèse Leccia[1]

[1]Laboratoire Oligoéléments et Résistance au Stress Oxydant induit par les Xénobiotiques (ORSOX; UMR UJF-CEA, LRC7 CEA 8 M), Université Joseph Fourier, UFR de Médecine et Pharmacie, La Tronche, France;
[2]Laboratoire des Lésions des Acides Nucléiques (LAN, SCIB/DRFMC), CEA, Grenoble Cedex, France;
[3]Département de Radiobiologie et de Radiopathologie, Centre de Recherche du Service de Santé Armées, La Tronche, France

Leccia Marie-Thérèse
Dermatologie, Département Pluridisciplinaire de Médecine
C.H.U. Albert Michallon
BP 217X
38043 Grenoble Cedex
France
Tel.: +33 476 76 93 19
Fax: +33 476 76 55 58
e-mail: mtleccia@chu-grenoble.fr

Introduction

Human papillomaviruses (HPV) are small double-strand DNA viruses that infect cutaneous or mucosal epithelia leading to benign proliferative lesions as warts or condylomas. Moreover, there is epidemiologic and molecular evidence that a subset of HPV, referred to as high-risk HPV, is associated with human anogenital cancers, such as cervical cancers (1). In addition to their role in the development of anogenital cancers, HPV are closely associated with the development of cutaneous cancers in patients with the rare inherited disease epidermodysplasia verruciformis (EV) (2). HPV have also been postulated in the development of non-melanoma skin cancers (NMSC) in both immunocompetent and immunocompromised people, such as organ transplant recipients (3,4). Two genes of high-risk HPV, E6 and E7 are regularly expressed in HPV-positive cancers and derived cell lines (5). E6 and E7 genes are both

necessary and sufficient for the efficient immortalization of primary human epithelial cells (6). The transforming activities of E6 and E7 are correlated, at least in part, with the inactivation of two cellular tumor-suppressor gene products, p53 and pRb (7–9). Interestingly, warts and skin cancers predominantly occur at body sites exposed to sunlight, suggesting possible interactions between HPV (and possibly E6 and E7 oncoproteins) and ultraviolet (UV) irradiation.

Solar UV radiation is the most important environmental factor involved in the pathogenesis of skin cancers (10). Harmful effects of UV radiation are associated both with direct DNA damage, through absorption energy, and with the generation of reactive oxygen species (ROS) directed against the various cellular components, such as DNA, membranes and proteins. The direct absorption energy by DNA results in the formation of DNA photoproducts, such as cyclobutane pyrimidine dimers (CPD), pyrimidine (4–6) pyrimidone photoproducts and their related Dewar valence isomers. In mammalian cells, the great majority of mutations induced by UV radiation result from unrepaired CPD (11). However, although these lesions are the best-studied type of UV-induced DNA damage, UV radiation induces a much wider range of DNA damage, such as protein–DNA cross-links, strand breaks, abasic sites and base modifications. Under UV radiation, oxidation of the guanine has been identified as the major base modification and it was formed 8-oxo-7,8-dihydro-2′deoxyguanosine(8-oxodGuo) (12–14). Although the role of these DNA lesions in UV-induced mutations seems to be minor, compared to CPD (12), their mutagenic potency should not be underestimated (13,14).

In order to protect against UV-induced oxidative stress, skin cells have developed complex antioxidant enzymatic and non-enzymatic defence systems, including superoxide dismutases (SOD), catalase, glutathione peroxidases (GSH-Px) and glutathione (GSH). Animal experiments and cultured cell studies have shown that GSH/GSH-Px pathway plays a major role in skin-cell protection against UV radiation (15,16).

Therefore, the aim of this study is to investigate the role of E6 and E7 oncoprotein levels on UV sensitivity and DNA damage of HPV type-16 cancer-derived cell lines in relation to the endogenous antioxidant status. Our experiments were performed *in vitro* by using two SKv keratinocyte lines, SKv-e and SKv-l. These cell lines were established from a bowenoid papulosis lesion, differing in the arrangement of HPV16 genome integration, expressing HPV16 E6 and E7 transforming proteins (17–19). They display different *in vitro* proliferative potential, which correlates with tumorigenicity in *nu/nµ* mice (20). We showed in this study that the highly tumorigenic cell line SKv-l, presented significantly higher E6* RNA levels, compared to SKv-e cell line. The higher expression of E6* RNA levels in SKv-l, compared to that in SKv-e, was associated with a high resistance to UV radiation and oxidative stress (as hydrogen peroxide, H_2O_2) and with low accumulation of oxidative-DNA damage in relation to a high GSH/GSH-Px content in these cells. These results suggest that HPV oncoprotein levels, in particular E6*, could modulate antioxidant status, particularly the GSH/GSH-Px pathway, to protect HPV-infected keratinocytes against an environmental oxidative stress.

Materials and methods

Chemicals

Eagle's minimum essential medium, foetal calf serum, gentamicin and normal melting agarose were purchased from Gibco (Life Technology Ltd, Paisley, Scotland). Fungizone was obtained from Bristol-Myers Squibb (Puteaux, France), hydrocortisone from Pharmacia & Upjohn SA (St Quentin-Yvelines, France) and low melting point agarose from FMC Bioproducts (Rockland, ME, USA). The RNA-PLUS solution was obtained from Q-Biogen (Illkirch, France), Reverse Transcription system from Promega Co. (Madison, WI, USA) and Micro BCA protein assay from Pierce (Rockford, IL, USA). LC Fast Start DNA Master SYBR Green kit was purchased from Roche Applied Science, Mannheim, Germany. Other reagents were purchased from Sigma Chemicals Co. (St Louis, MO, USA).

Cell culture

SKv keratinocyte lines (SKv-e and SKv-l) were the generous gifts from F. Breitburd and G. Orth from the Pasteur Institute. These cell lines were established from a bowenoid papulosis lesion. They harboured 10–20 copies of HPV16 genome integrated within a single site in region q14–q15 of chromosome-12 and expressed HPV16 E6 and E7 transforming proteins (17–19). After *in vitro* passaging, the two distinct SKv cell variants, SKv-e and SKv-l, were derived, differing in the arrangement of HPV16 genome integration (17). Likewise, SKv cell lines were well characterized for their proliferative and tumorigenic capacities (20).

SKv cells were grown in Eagle's minimum essential medium supplemented with 20% foetal calf serum, 10^{-6} M hydrocortisone, 100 µg/ml of gentamicin and 2.5 µg/ml of fungizone.

RNA extraction and quantitative reverse transcription-polymerase chain reaction (RT-PCR) analysis

RNA extraction and RT. Total RNA was extracted by a simplified and improved modification of the Chomczynski's procedure with the RNA-PLUS solution according to the manufacturer's protocols. Total RNA (1 µg) was reverse-transcribed by using the Reverse Transcription System: the RT reaction (20 µl) was primed with both oligo(dT)$_{15}$ (0.5 µg)

and specific E6 and E7 primers (0.05 μM; HPV16.E6 5′-ATG-CATGATTACAGCTGGGT-3′; HPV16.E7 5′-CAGCCATGG-TAGATTATGGT-3′) and was then incubated for 15 min at 42°C.

Quantitative PCR analysis. Primer design and optimization regarding dimerization, self-priming and melting temperature were performed by using MacVector software (Accelrys, San Diego, CA, USA). The size of PCR products was controlled by means of Agilent 2100 Bioanalyzer with DNA 500 Assay (Agilent Technology, Waldbronn, Germany). In addition, specificities of PCR products were checked with melting curve analysis (Light-cycler Software v.3.5., Roche Applied Science). Forward E6* primer spans the splicing region of the truncated E6 product. PCR were performed both from RT products and from specific recombinant DNA overlapping PCR products. Melting peaks obtained either from RT products or from specific recombinant DNA were identical (21). For E6* and E7 RT products, single melting peaks were obtained.

All primers used in this study were synthesized at Proligo Primers & Probes (France). The PCR was performed with the LC Fast Start DNA Master SYBR Green kit by using 0.5 μl of cDNA (equivalent to 25 ng of total RNA) in a 20 μl final volume, 4 mM $MgCl_2$ and 0.4 μM of each primer (final concentration). Quantitative PCR was performed by using a Lightcycler (Roche Applied Science) for 35 cycles at 95°C for 20 s, 56°C (E6*), 58°C (peptidylpropyl isomerase A, PPIA) or 60°C (E7 and hypoxanthine phosphoribosyltransferase 1, HPRT1) for 5 s, and a final step of 10 s at 72°C. Viral oncogene expression was normalized by means of geometric averaging of two internal control genes, *PPIA* and *HPRT1* (22). Quantification was achieved with the comparative threshold cycle method (23) by using RealQuant Software (Roche Applied Science).

The primers used were E6-forward 5′-CCAGAAAGTTACCA-CAGTTATG-3′, E6-reverse 5′-ATCCCGAAAAGCAAAGTC-3′, E6*-forward 5′-CAGTTACTGCGACGTGAG GTGTAT-3′, E6*-reverse 5′-CCACCGACCCCTTATATTATGGA-3′, E7-for-ward 5′-TGCGTACAAAGCACACACGTAGA-3′, E7-reverse 5′-AGATGGGGCACACAATTCCTAGT-3′, PPIA-forward 5′-C A TCTGCACTGCCAAGACTGAGTG-3′, PPIA-reverse 5′-CTTCTTGCTGGTCTTGCCATTCC-3′, HPRT1-forward 5′-C TCATGGACTAATTATGGACA GGAC-3′ and HPRT1-reverse 5′-GCAGGTCAGCAAAGAATTTATAGCC-3′.

UV sources and irradiation procedure

Solar-simulated radiation (SSR) source. The light source used was a Dermolum UM-W (Müller GmbH Elektronik-optik, Moosinning, Germany) equipped with a 1-kW Xenon Lamp and a water filter. The UV spectrum was obtained by passing light through a 1-mm WG305 filter (Müller GmbH Elektronik-optik). This filtered Xenon source provided a simulated solar UVR spectrum that nearly eliminated visible and infrared radiation. The irradiance effectively received by the cells (22.5 mW/cm^2) was measured by using a dosimeter (Müller GmbH Elektronik-optik) with a spectral sensitivity from 270 nm to 4 μm.

UVB source. The UVB light source used was a T-40M apparatus equipped with three 40 W fluorescent tubes (Vilbert-Lourmat, Torcy, France), with a spectrum distribution of 280–320 nm, and $\lambda_{max} = 312$ nm. Radiation fluxes were measured by means of an international light radiometer (RX, Vilbert-Lourmat). The apparatus was controlled with the help of a microprocessor monitoring the time of irradiation according to the desired energy.

UVA source. The UVA source used was a Waldmann UVA 700L fitted with an MSR 700 (700 W) lamp with a spectrum distribution of 320–490 nm, and with $\lambda_{max} = 365$ nm. The irradi-ance effectively received by the cells was 80 mW/cm^2 (measured by using a dosimeter).

Irradiation procedure. Practically, cells were irradiated with various physiological UV doses. Just before irradiation, the culture medium was removed and was reserved. Cells were rinsed twice with 1 ml of phosphate-buffered saline (PBS) without cal-cium and magnesium. Irradiations were performed through 1 ml of PBS, which is UV inert, lid removed. Control cells were similarly treated and were left in the dark while irradiation was performed. After the stress, cells were put back into their initial medium and were placed in the incubator for an appropriate recovery period depending on the type of experiments.

Hydrogen peroxide stress

Sub-confluent cells were treated with various H_2O_2 concentra-tions. Practically, just before the stress, the culture medium was removed and was reserved. Cells were rinsed twice with 1 ml of PBS. Then the cells were treated with 1 ml of H_2O_2 diluted in PBS for 30 min in the dark at room temperature. The final H_2O_2 concentrations were varying from 0 to 30 mM. Control cells were kept in PBS under the same environmental conditions. After the stress, cells were rinsed twice again with 1 ml of PBS; they were put back into their initial medium and were placed in the incubator for 24 h.

Cell viability assay

The cell viability was determined by using the conversion of the tetrazolium salt, 3-(4,5-dimethylthiazol-2-yl)-2,5-diphenyl tetra-zolium bromide (MTT), to formazan by the metabolically active cells. Twenty-four hours after irradiation or hydrogen peroxide treatment, 200 μl of 5 mg/ml MTT was added in each dish and cells were incubated for 2 h at 37°C. DMSO was then added in order to dissolve the soluble blue formazan and the absorbance at 570 nm was measured by means of spectrophotometry. The results represent the means of at least three measurements with three Petri dishes for each condition. The results were expressed as the percentage of viability calculated from the formula [(A–B)/(C–B)] × 100 where A = OD_{570} of the treated cells, B = OD_{570} of the medium and C = OD_{570} of the control cells.

Biochemical analysis

Under basal conditions, sub-confluent cells were trypsinized and were washed three times in isotonic 175 mM Tris–HCl buffer, pH 7.30. Then, cells were lysed in hypotonic 8.75 mM Tris–HCl buffer by five freeze-defrost cycles. The resulting homogenates were either reserved for total GSH measurement or centrifuged for 10 min at 4000 rpm at 4°C. The supernatants were stored at −80°C until metalloenzyme analysis.

Metalloenzyme activities. The GSH-Px activity was deter-mined as previously described by using ter-butyl hydroperoxide as substrate (16). This was achieved by following the decrease in nicotinamide adenine dinucleotide phosphate (NADPH) concen-tration at 340 nm. Results were expressed as micromoles of NADPH oxidized per minute.

Catalase activity was determined by means of the decomposi-tion of H_2O_2 at 240 nm as previously described (24). One unit of catalase is defined as 1 μmol of H_2O_2 consumed per minute.

Manganese SOD (Mn SOD) and copper–zinc SOD (Cu–Zn SOD) activities were determined using the method of Marklund and Marklund by monitoring the rate of the oxidation of pyrogallol by superoxide radicals (25). The specific inhibition of Cu–Zn SOD by 9 mM potassium thiocyanate allows Mn SOD

determination by the same procedure as previously described (26). Results were expressed as SOD units (1 U is the amount of SOD inhibiting the reaction rate by 50% in the given assay conditions).

Enzymatic activities were normalized to the soluble cell protein content determined by using the Micro BCA protein assay. The result of at least three replicate experiments was given.

Total GSH measurement. Cell homogenates were immediately deproteinized by adding 6% metaphosphoric acid (lysate/metaphosphoric acid, 5/1, v/v). Total GSH was determined by using 5,5′-dithiobis-2-nitrobenzoic acid as previously described (27). GSH levels were normalized to the total cell protein content determined by means of the Micro BCA protein assay.

Alkaline single-cell gel electrophoresis (comet assay)

DNA damage was evaluated using the Comet assay that allows the measurement of single- and double-strand breaks together with alkali-labile sites. The procedure previously described (28) was slightly modified as follows. Typically, $150 \mu l$ of 0.5% normal melting agarose in PBS buffer was dropped on frosted microscope slides (Touzart et Matignon, Les Ullis, France), covered with a cover slip, and kept at room temperature until their subsequent use. After trypsination, SKv-e and SKv-l cells were washed twice with PBS, and the cell pellets were suspended in PBS. About 20 000 cells in $60 \mu l$ were mixed with an equal volume of 1.2% low melting point agarose in PBS buffer, held at $37°C$. Embedded cells were immediately irradiated with SSR. Then, all slides were immersed overnight in lysis buffer ($2.5 mM$ NaCl, $100 mM$ EDTA, $100 mM$ Tris, 10% sodium lauroyl sarcosinate, 1% triton X-100, 10% DMSO, pH 10) in the dark at $4°C$ in order to limit non-specific DNA damage to occur. After lysis, the *Escherichia coli* formamidopyrimidine DNA N-glycosylase (Fpg) was used in order to convert purine base modifications into single-strand breaks. Slides were washed one time for $10 min$ with neutralization buffer ($0.4 M$ Tris–HCl, pH 7.5), three times for $10 min$ with Fpg buffer ($0.1 M$ KCl, $0.5 mM$ Na_2EDTA and $40 mM$ Tris, adjusted to pH 8). Then $100 \mu l$ of $1 \mu g/ml$ of Fpg was laid on the slides, before incubation at $37°C$ for $45 min$ in a humidified atmosphere. Slides were then placed in a horizontal electrophoresis unit containing freshly alkaline buffer ($1 mM$ EDTA and $300 mM$ NaOH) for $40 min$ to allow the unwinding of the DNA. Electrophoresis was performed at $25 V$ and $300 mA$ for $30 min$. Then, the slides were rinsed three times for $5 min$ with neutralization buffer; they were stained with $50 \mu l$ of ethidium bromide ($20 \mu g/ml$) and were covered with a cover slip. Slides were placed in a humidified airtight container in order to prevent drying of the gel, until the analysis was performed.

DNA damage was quantitated by means of the image analysis system Komet 3.0 (Kinetic Imaging, Liverpool, UK). The quantification of DNA damage was performed by using the tail moment, the product of the tail distance (i.e. the distance between the centre position of the head and the centre gravity of the tail) and the percentage of the DNA in the tail (relative to the total amount of DNA in the entire comet (head + tail)). For each condition, 50 randomly selected comets on each slide were scored and the averaged tail moment was determined using three slides prepared as described.
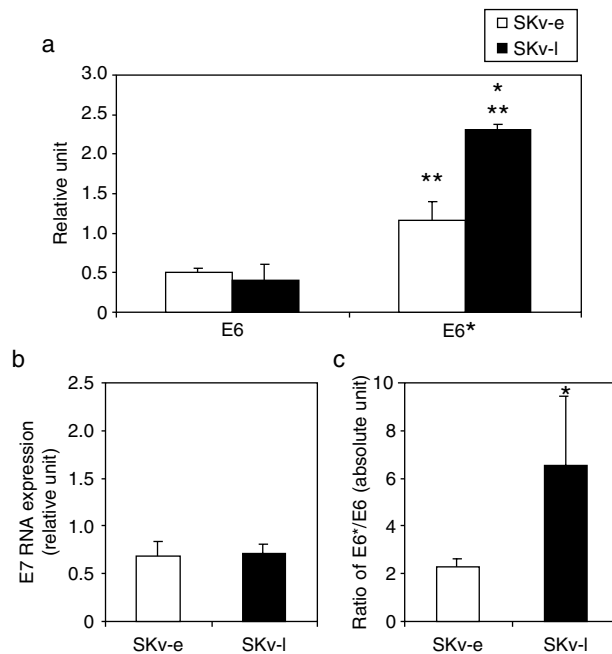
Statistical analysis

Each experiment was repeated at least three times. All data expressed as mean ± SD were processed by statistically using one way analysis of variance (ANOVA) and Newman-Keuls test. Differences were considered significant when $P < 0.05$.

Results

Different E6* RNA expression in SKv cell lines

SKv-e and SKv-l were two distinct keratinocyte variants harbouring HPV16 genome and expressing E6 and E7 transforming proteins. The E6/E7 coding region of HPV16 is known to be alternatively spliced within the E6 open reading frame resulting in full-length E6 and its truncated forms E6* and E6**. These cell lines have been shown to display different proliferative potential correlated with different tumorigenicity in mice, suggesting a possible difference in E6, and truncated forms, and E7 expression levels. We studied E6 and E7 RNA expression in SKv cell lines by means of quantitative RT-PCR. For E6, E6* and E7 RT-PCR products, a single melting peak was obtained in the two cell lines and the size of PCR products was controlled by using Agilent 2100 Bioanalyzer (data not shown). Figure 1 shows the different expression of E6, E6* and E7 transcripts in the two cell lines. In particular, we showed in Fig. 1a that the amount of E6* RNA was significantly higher than E6 RNA in the two cell lines ($P < 0.0006$). The expression of E6* RNA

Figure 1. **E6, E6* and E7 RNA transcript expression in SKv cells.** HPV RNA transcript expression was assayed by means of quantitative RT-PCR as described in the section entitled 'Materials and methods.' Results represent averages from three independent experiments. (a) E6 and E6* RNA transcript expression, *$P < 0.0002$, SKv-l vs SKv-e; **$P < 0.0006$ E6* vs E6. (b) E7 RNA transcript expression. (c) Ratio of E6* and E6 in SKv cells; *$P < 0.04$, SKv-l vs SKv-e. HPV, human papillomavirus; RT-PCR, reverse transcription-polymerase chain reaction.

transcript was two-fold higher in SKv-l, compared to that in SKv-e: 2.31 ± 0.06 and 1.16 ± 0.24, respectively ($P < 0.0002$, Fig. 1a), whereas the expression of E6 RNA transcript was similar in the two cell lines. Therefore, the ratio E6*/E6 was 2.31 ± 0.33 in SKv-e and 6.53 ± 2.93 in SKv-l (Fig. 1c). Concerning E7 transcripts, no difference was observed between the two cell lines (Fig. 1b).

SKv cell lines display different cell survival after solar-simulated irradiation

SKv-e and SKv-l cell lines were exposed to increasing SSR doses and cytotoxicity was evaluated by using the MTT assay 24 h after the stress. In the two cell lines, cytotoxicity increased with increasing SSR irradiation in a dose-dependent manner (Fig. 2). However, SKv-e cells were significantly more sensitive than SKv-l cells to SSR with a lethal dose of 50 (LD_{50}) of $0.6 \, J/cm^2$ for SKv-e cell line and of $1.5 \, J/cm^2$ for SKv-l cells ($P < 0.001$).

SKv cell lines display different cell survival after UV irradiation

Considering the difference of cell survival, observed between the two SKv cell lines under SSR, we studied the specific effects of UVB or UVA spectrum on cell cytotoxicity. SKv-e and SKv-l keratinocytes were exposed to increasing UVA (Fig. 3a) or UVB (Fig. 3b) irradiation doses. Figure 3a shows that, in the two cell lines,
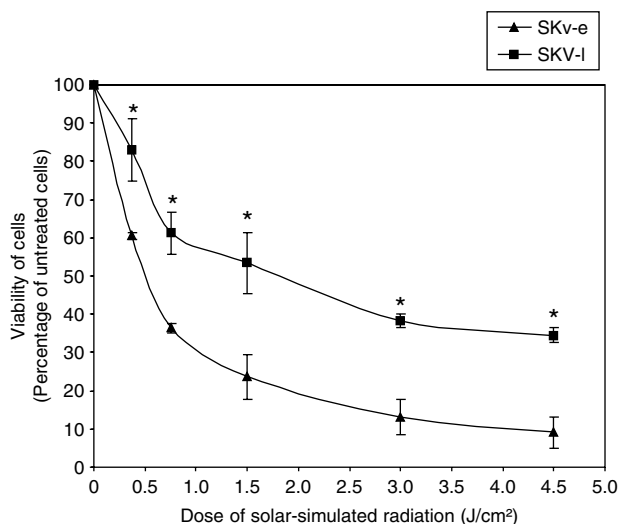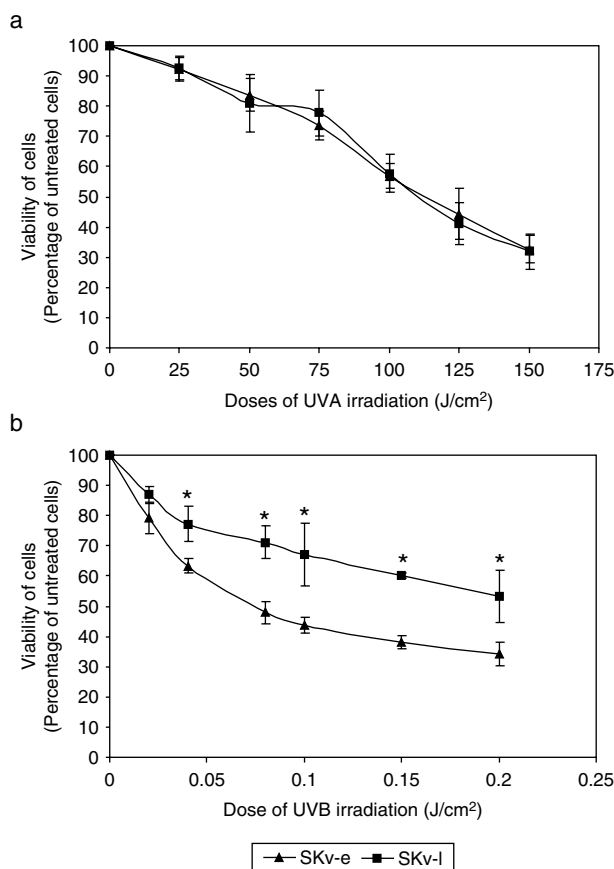
Figure 3. Cell survival of SKv cells treated with ultraviolet-A (UVA) or UVB. Viability was assessed 24 h after UV irradiation by using the MTT assay. Values represent averages from at least three independent experiments and are normalized to the amount of viable cells remaining in untreated culture cells. (a) Cell survival of SKv cells treated with UVA. (b) Cell survival of SKv cells treated with UVB, *$P < 0.013$, SKv-l vs SKv-e.

cytotoxicity increased with increasing UVA irradiation doses from 0 to $150 \, J/cm^2$ with a similar LD_{50} of $100 \, J/cm^2$ for SKv-e and SKv-l cells.

UVB cytotoxicity increased also in a dose-dependent manner with increasing UVB irradiation doses in the two SKv cell lines (Fig. 3b). However, like for SSR, differences of sensitivity were observed for SKv-e and SKv-l, as LD_{50} was $0.08 \, J/cm^2$ for SKv-e and $0.2 \, J/cm^2$ for SKv-l ($P < 0.013$).

Differences in GSH levels and GSH-Px activities between SKv-e and SKv-l cell lines

We postulated that differences in SSR and UVB sensitivity of SKv cells could result from different antioxidant status. Therefore, we evaluated GSH contents, SOD, catalase and GSH-Px activities in the two SKv cell lines (Table 1). SKv-l cell line, the most resistant cells to SSR and UVB irradiation, had total GSH levels three-fold higher than SKv-e cell line: 76.98 and $26.25 \, \mu mol/g$ of total proteins,

Figure 2. Cell survival of SKv cells treated with solar-simulated radiation (SSR). Viability was assessed 24 h after SSR by using the MTT assay. Results are expressed as percentage viability, with 100% viability for untreated cells. Values represent averages from at least three independent experiments. *$P < 0.001$, SKv-l vs SKv-e.

Table 1. Antioxidant content in SKv cells under basal conditions

	SKv-l	SKv-e
GSH-Px (U/g of soluble proteins)	197.61 ± 43.03[1]	78.98 ± 14.25
Catalase (U/mg of soluble proteins)	5.20 ± 1.92	2.85 ± 1.03
Total SOD (U/mg of soluble proteins)	6.36 ± 0.52	6.78 ± 1.20
Mn SOD (U/mg of soluble proteins)	2.99 ± 0.45	2.94 ± 1.09
Cu–Zn SOD (U/mg of soluble proteins)	3.37 ± 0.07	3.84 ± 0.10
Total GSH (μmol/g of total proteins)	76.98 ± 11.81[2]	26.25 ± 1.01

Metalloenzyme activities and total GSH levels were determined as described in the section entitled 'Materials and methods.' Results are expressed as mean ± SD from at least three independent experiments.
[1] $P < 0.02$, SKv-l vs SKv-e.
[2] $P < 0.03$, SKv-l vs SKv-e.
GSH, glutathione; GSH-Px, glutathione peroxidase; SOD, superoxide dismutases.

respectively ($P < 0.02$). Furthermore, GSH-Px, an enzyme involved in peroxide detoxification by using GSH as substrate, had activities 2.5-fold higher in SKv-l, compared to those in SKv-e: 197.61 vs 78.98 U/g of soluble proteins, respectively ($P < 0.03$). Catalase activity was slightly, but not significantly, higher in SKv-l, compared to that in SKv-e. No difference was found between the two cell lines for total SOD, Cu–Zn SOD and Mn SOD activities, enzymes involved in superoxide anion dismutation.

SKv cells display different H_2O_2 sensitivity

Considering the differences observed for GSH levels and GSH-Px activities between the two SKv cell lines, we postulated that H_2O_2 production under SSR and UVB irradiation could explain the different cytotoxicity observed in SKv-e and SKv-l cells.

H_2O_2 treatment decreased SKv cell survival in a dose-dependent manner (Fig. 4). Our results showed that, like for SSR and UVB irradiation, SKv-e were significantly more sensitive to H_2O_2 treatment than SKv-l: LD_{50} was obtained with 11 mM for SKv-e and 16 mM for SKv-l showing a higher sensitivity of SKv-e cell lines to H_2O_2-induced oxidative stress ($P < 0.0011$).

SSR induced different oxidative DNA damage formation in SKv cells

UV-induced DNA damage is critical for the control of cell survival and cell proliferation. Considering the differences observed between SKv-e and SKv-l cell cytotoxicity and antioxidant status, we postulated that various levels of DNA damage could be induced in the two cell lines under SSR. Therefore, genotoxic effects of a single SSR ($0.5 \, J/cm^2$) were evaluated by using the comet assay immediately after irradiation (Fig. 5). Under basal condition,

no difference in tail moment was observed between the two cell lines, indicating no difference in total DNA damage between SKv cells; tail moment was 9.0 ± 0.2 for SKv-e and 8.8 ± 0.7 for SKv-l. Compared to sham-irradiated cells, irradiated cells ($0.5 \, J/cm^2$) showed a three-fold increase of the tail moment ($P < 0.003$), indicating that SSR generated direct strand breaks and/or alkali-labile sites. But no difference of the tail moment was observed between irradiated SKv-e and SKv-l cell lines; tail moment was 24.5 ± 1.8 for SKv-e and 27.0 ± 4.0 for SKv-l.

Assuming the fact that the difference in the survival of SKv-irradiated cells resulted from an oxidative stress as previously hypothesized, we evaluated oxidative DNA damage formation by using the DNA-glycosylase Fpg, enzyme involved in the removal of modified purine bases. As shown in Fig. 5, the tail moment determined in sham-irradiated cells treated with Fpg (1 μg/ml) was three-fold higher than in the absence of glycosylase ($P < 0.0021$). But no difference was observed between sham-irradiated SKv-e and SKv-l cells; tail moment was 27.4 ± 3.3 and 28.3 ± 3.3, respectively. The tail moment, measured using this modified comet assay, strongly increased in SSR-irradiated SKv-e and SKv-l cells, confirming that oxidative DNA damage was generated by means of SSR ($P < 0.003$). Using this modified comet assay, the tail moment showed a 3.5-fold increase in the SKv-e-irradiated cells and a 2.7-fold increase in the SKv-l-irradiated cells; tail moment
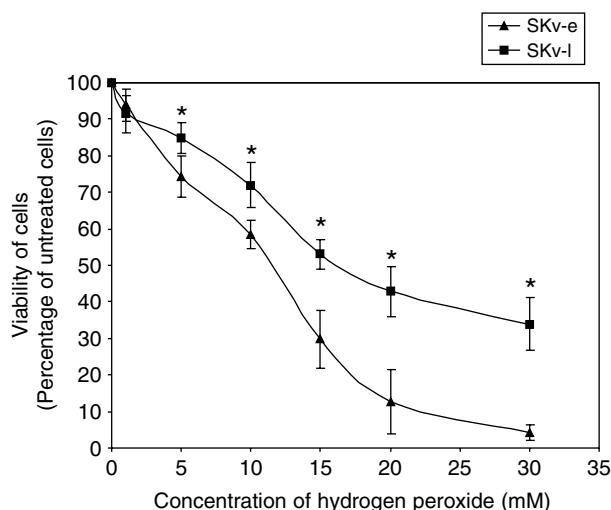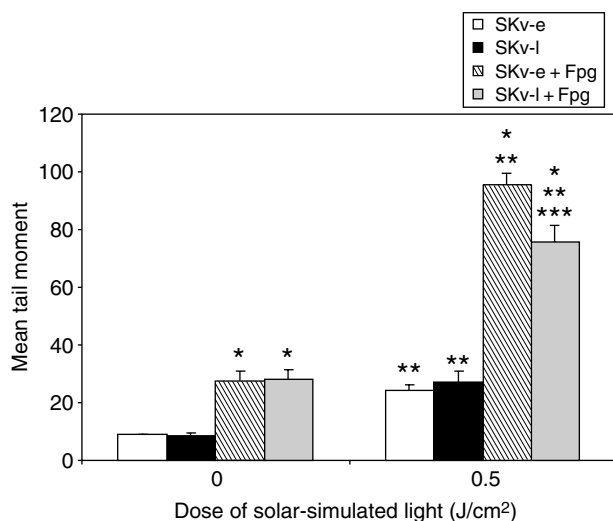

Figure 4. **Cell survival of SKv cells treated with increasing concentrations of hydrogen peroxide.** Viability was assessed 24 h after H_2O_2 treatment by using the MTT assay. Values represent averages from at least three independent experiments and are normalized to the amount of viable cells remaining in untreated cells. *$P < 0.0011$, SKv-l vs SKv-e.

Figure 5. Evaluation of DNA damage in SKv cells after a single dose of solar-simulated radiation (SSR). DNA damage was assessed immediately after SSR by using the comet assay with or without formamidopyrimidine DNA *N*-glycosylase (Fpg). Results are expressed as mean tail moment and represent the mean of at least three independent assays. *$P < 0.0021$, cells with Fpg *vs* cells without Fpg; **$P < 0.003$, irradiated cells with and without Fpg *vs* non-irradiated cells with and without Fpg; ***$P < 0.002$, irradiated SKv-l cells with Fpg *vs* irradiated SKv-e cells with Fpg.

was 95.6 ± 4.1 for SKv-e and 75.8 ± 5.5 for SKv-l. These results showed that SKv-e cell line accumulated significantly much more oxidative DNA damage than SKv-l cell line ($P < 0.002$).

Discussion

HPV are small circular DNA viruses that are confined to the epithelial cells of both mucosa and skin. There is overwhelming epidemiological evidence that high-risk HPV types infecting the genital mucosa play a crucial role in the development of cervical dysplasia and carcinoma. Cellular and molecular biological studies confirmed these epidemiological data by demonstrating that E6/E7 oncoproteins are the main determinants of the malignant phenotype in those cervical carcinoma cells (1).

A role for HPV in the development of NMSC has also been postulated. The earliest evidence for the involvement of HPV in human skin cancers has resulted from observations of patients suffering from EV disease (2). EV-associated HPV have then been detected in premalignant skin lesions and NMSC of immunocompetent and immuno-compromised patients, particularly organ transplant recipients (3,4,29–31). In NMSC of these patients, both cutaneous and mucosal HPV types

have been detected by means of PCR techniques (3,4). NMSC are preferentially developed at sun-exposed sites, suggesting that HPV could act as co-factors with UV irradiation to transform cutaneous keratinocytes and then contribute to the carcinogenic process. In this way, it has been shown that the promoter activity of HPV77, HPV only found in skin cancers, was stimulated by UV irradiation via a p53 mechanism, which increased the expression level of E7 oncoprotein (32). Moreover, E6 of both cutaneous and mucosal HPV has been shown to inhibit both p53-dependent and p53-independent apoptosis in response to UV irradiation (33). However, as cutaneous HPV can not immortalize and transform skin cells *in vitro*, these data obtained from transfection studies may have resulted in high protein expression levels and could not be biologically relevant.

In our study, we used two HPV16-infected keratinocyte lines, SKv-e and SKv-l, well characterized for their proliferative and tumorigenic capacities. It is, today, admitted that, in human tumours and in derived cell lines infected with high-risk HPV, E6 and E7 RNA are produced as full-length transcripts and spliced forms of E6. RT-PCR is, generally, the best technique employed in order to determine HPV transcript production in HPV-infected cell lines (34). We showed by means of quantitative RT-PCR that the highly tumorigenic SKv-l cell line presented significantly higher E6* RNA levels, compared to SKv-e cell line. By contrast, we did not find any difference in E6 and E7 RNA levels between the two cell lines. Interestingly, we demonstrated that the higher expression of E6* RNA levels in SKv-l, compared to that in SKv-e, was associated with a high resistance to SSR and more specifically to UVB radiations.

The potential to encode E6* proteins is an exclusive property of high-risk HPV types, but attempts to demonstrate that these oncoproteins possess transforming activity were unsuccessful (35). Pim and Banks have shown that HPV18 E6* protein was able to interact with both the full-length E6 and the E6-AP proteins *in vitro* and thereby to block the association of E6 with p53 (36). However, the biological function of E6* protein remains to be clarified, but it does suggest a fine-tuning of oncoprotein activity and a complex interplay between E6, E6* and cellular target proteins, particularly p53, during viral infection. Our results, showing a high expression of E6* transcript, compared to that of E6 and E7, in SKv cells and a higher expression of E6* RNA in the more tumorigenic cell line, SKv-l, underlie the

potential importance of E6* in HPV-induced cell transformation.

After UV-induced DNA damage, p53 plays a key role as is able to arrest cell cycle in order to allow time to repair DNA damage, or to direct damaged cells to an apoptotic pathway. *In vitro* studies have shown that E6 and E7 proteins of high-risk HPV have the ability to interact with cell cycle proteins, such as p53 and p21, and to disrupt cell cycle control (7,37–39). Therefore, at this time, we are investigating p53 and p21 expression and apoptosis in SKv cell lines in response to UV irradiation in order to determine the role of HPV oncoprotein levels in keratinocyte cell cycle modifications.

Harmful effects of solar UV radiation are associated with both direct damage and generation of ROS against the different cellular components. In addition to its direct effect, it has also been shown that UVB can induce ROS, particularly H_2O_2, and by this way can modulate signaling pathways, transcriptional activation (40–42) and apoptotic cell death (43,44). Moreover, as after UVA radiation, oxidative DNA damage is also generated after UVB irradiation (45).

The comet assay allows the measurement of strand breaks, abasic sites and base modifications. Interestingly, we showed with this method that the most sensitive SKv-e cell line to SSR and UVB accumulated significantly much more oxidative DNA damage after SSR than SKv-l cell line. This result suggests that the differences observed in SSR and UVB cell survival could result from an oxidative stress and different oxidative DNA damage accumulations.

The mutagenic potency of oxidative DNA damage, particularly 8-oxodGuo, participates in the carcinogenic process (13,14) and is correlated with the grade of cervical dysplasia (46). Interestingly, it has also been shown that HPV oncoproteins could alter p53-dependent DNA damage repair (47,48). However, in these studies, results were obtained by means of transfection techniques that may have resulted in very high oncoprotein expression levels. Therefore, at this time, we are investigating DNA photoproducts and 8-oxodGuo accumulation and repair induced by SSR in the two SKv cell lines in order to determine the role of HPV oncoprotein levels in the formation of mutations, which are known to be critical in carcinogenesis.

Assuming the fact that differences observed in the survival of SSR- and UVB-irradiated cells could result from an oxidative stress, we postulated that SKv cell lines could present different antioxidant status. Under basal condition, we demonstrated that SKv-l, the most resistant cells to SSR and UVB irradiation, had total GSH levels and GSH-Px activities, which were significantly higher than those of SKv-e cells. As GSH-Px is an enzyme involved in peroxide detoxification by using GSH and considering the fact that UVB irradiation produces H_2O_2, we studied the sensitivity of SKv cell lines to H_2O_2 treatment. Interestingly, like for SSR and UVB irradiation, we demonstrated that the higher GSH levels and GSH-Px activities in SKv-l, compared to those in SKv-e cells, were associated with a higher resistance to H_2O_2 treatment. Therefore, in view of these results, we concluded that, in our model, H_2O_2 plays an essential role and appears to be the most important mediator of the UV irradiation-induced cytotoxicity. We can also hypothesize that in our cellular model, UVB radiation is a more powerful inductor of H_2O_2 than UVA radiation. We also demonstrated the importance of the couple GSH/GSH-Px, which plays an essential role in H_2O_2 and peroxide detoxification, and then in protecting cells from UV-induced oxidative damage.

In our model, high levels of GSH contents and GSH-Px activities are associated with high E6* RNA expression levels. Previous studies have shown that several DNA or RNA viruses are able to modulate GSH-Px expression and activities (49,50). By this way, theses viruses protect infected cells against cytotoxic effects induced by environmental stress (51). Therefore, the results of our study suggest that HPV E6* oncoprotein levels could modulate the GSH/GSH-Px pathway to protect HPV-infected keratinocytes against an environmental oxidative stress, such as solar radiation. Complementary studies will be necessary in order to confirm this attractive hypothesis.

Moreover, it is known that in cancer cells, GSH contents and GSH-Px activities are, most of the time, significantly enhanced, compared to normal tissues, suggesting the involvement of the GSH/GSH-Px pathway in malignant cell resistance to oxidative stress (52,53). In transgenic mice, the overexpression of skin antioxidant enzymes, GSH-Px or GSH-Px and SOD, leads to an increase, rather than a decrease of skin carcinogenesis (54). In conclusion, GSH/GSH-Px pathway seems to be an antioxidant mechanism of first importance in HPV-infected keratinocyte survival and HPV-associated carcinogenic process.

References

1. zur Hausen H. Papillomavirus infections – a major cause of human cancers. Biochim Biophys Acta 1996: 1288: F55–F78.

2. Orth G, Jablonska S, Jarzabek-Chorzelska M et al. Characteristics of the lesions and risk of malignant conversion associated with the type of human papillomavirus involved in epidermodysplasia verruciformis. Characterization of two types of human papillomaviruses in lesions of epidermodysplasia verruciformis. Cancer Res 1979: 39: 1074–1082.

3. Harwood C A, Surentheran T, McGregor J M et al. Human papillomavirus infection and non-melanoma skin cancer in immunosuppressed and immunocompetent individuals. J Med Virol 2000: 61: 289–297.

4. Biliris K A, Koumantakis E, Dokianakis D N, Sourvinos G, Spandidos D A. Human papillomavirus infection of non-melanoma skin cancers in immunocompetent hosts. Cancer Lett 2000: 161: 83–88.

5. Seedorf K, Oltersdorf T, Krammer G, Rowekamp W. Identification of early proteins of the human papilloma viruses type 16 (HPV 16) and type 18 (HPV 18) in cervical carcinoma cells. EMBO J 1987: 6: 139–144.

6. Munger K, Phelps W C, Bubb V, Howley P M, Schlegel R. The E6 and E7 genes of the human papillomavirus type 16 together are necessary and sufficient for transformation of primary human keratinocytes. J Virol 1989: 63: 4417–4421.

7. Werness B A, Levine A J, Howley P M. Association of human papillomavirus types 16 and 18 E6 proteins with p53. Science 1990: 248: 76–79.

8. Scheffner M, Werness B A, Huibregtse J M, Levine A J, Howley P M. The E6 oncoprotein encoded by human papillomavirus types 16 and 18 promotes the degradation of p53. Cell 1990: 63: 1129–1136.

9. Dyson N, Howley P M, Munger K, Harlow E. The human papilloma virus-16, E7 oncoprotein is able to bind to the retinoblastoma gene product. Science 1989: 243: 934–937.

10. Armstrong B K, Kricker A. The epidemiology of UV induced skin cancer. J Photochem Photobiol B 2001: 63: 8–18.

11. You Y H, Lee D H, Yoon J H, Nakajima S, Yasui A, Pfeifer G P. Cyclobutane pyrimidine dimers are responsible for the vast majority of mutations induced by UVB irradiation in mammalian cells. J Biol Chem 2001: 276: 44688–44694.

12. Douki T, Perdiz D, Grof P et al. Oxidation of guanine in cellular DNA by solar UV radiation: biological role. Photochem Photobiol 1999: 70: 184–190.

13. Ahmed N U, Ueda M, Nikaido O, Osawa T, Ichihashi M. High levels of 8-hydroxy-2'-deoxyguanosine appear in normal human epidermis after a single dose of ultraviolet radiation. Br J Dermatol 1999: 140: 226–231.

14. Hattori Y, Nishigori C, Tanaka T et al. 8-hydroxy-2'-deoxyguanosine is increased in epidermal cells of hairless mice after chronic ultraviolet B exposure. J Invest Dermatol 1996: 107: 733–737.

15. Hanada K, Sawamura D, Tamai K, Hashimoto I, Kobayashi S. Photoprotective effect of esterified glutathione against ultraviolet B-induced sunburn cell formation in the hairless mice. J Invest Dermatol 1997: 108: 727–730.

16. Leccia M T, Richard M J, Beani J C et al. Protective effect of selenium and zinc on UV-A damage in human skin fibroblasts. Photochem Photobiol 1993: 58: 548–553.

17. Schneider-Maunoury S, Croissant O, Orth G. Integration of human papillomavirus type 16 DNA sequences: a possible early event in the progression of genital tumors. J Virol 1987: 61: 3295–3298.

18. Schneider-Maunoury S, Pehau-Arnaudet G, Breitburd F, Orth G. Expression of the human papillomavirus type 16 genome in SK-v cells, a line derived from a vulvar intraepithelial neoplasia. J Gen Virol 1990: 71: 809–817.

19. Sastre-Garau X, Schneider-Maunoury S, Couturier J, Orth G. Human papillomavirus type 16 DNA is integrated into chromosome region 12q14-q15 in a cell line derived from a vulvar intraepithelial neoplasia. Cancer Genet Cytogenet 1990: 44: 243–251.

20. Malejczyk J, Malejczyk M, Majewski S et al. Increased tumorigenicity of human keratinocytes harboring human papillomavirus type 16 is associated with resistance to endogenous tumor necrosis factor-alpha-mediated growth limitation. Int J Cancer 1994: 56: 593–598.

21. Peinnequin A, Mouret C, Birot O et al. Rat pro-inflammatory cytokine and cytokine related mRNA quantification by real-time polymerase chain reaction using SYBR green. BMC Immunol 2004: 5: 3.

22. Vandesompele J, De Preter K, Pattyn F et al. Accurate normalization of real-time quantitative RT-PCR data by geometric averaging of multiple internal control genes. Genome Biol 2002: 3: RESEARCH0034.

23. Livak K J, Schmittgen T D. Analysis of relative gene expression data using real-time quantitative PCR and the 2(-Delta Delta C(T)) method. Methods 2001: 25: 402–408.

24. Richard M J, Guiraud P, Didier C, Seve M, Flores S C, Favier A. Human immunodeficiency virus type 1 Tat protein impairs selenoglutathione peroxidase expression and activity by a mechanism independent of cellular selenium uptake: consequences on cellular resistance to UV-A radiation. Arch Biochem Biophys 2001: 386: 213–220.

25. Marklund S, Marklund G. Involvement of the superoxide anion radical in the autoxidation of pyrogallol and a convenient assay for superoxide dismutase. Eur J Biochem 1974: 47: 469–474.

26. Parat M O, Richard M J, Leccia M T, Amblard P, Favier A, Beani J C. Does manganese protect cultured human skin fibroblasts against oxidative injury by UVA, dithranol and hydrogen peroxide? Free Radic Res 1995: 23: 339–351.

27. Emonet N, Leccia M T, Favier A, Beani J C, Richard M J. Thiols and selenium: protective effect on human skin fibroblasts exposed to UVA radiation. J Photochem Photobiol B 1997: 40: 84–90.

28. Emonet-Piccardi N, Richard M J, Ravanat J L, Signorini N, Cadet J, Beani J C. Protective effects of antioxidants against UVA-induced DNA damage in human skin fibroblasts in culture. Free Radic Res 1998: 29: 307–313.

29. Tieben L M, Berkhout R J, Smits H L et al. Detection of epidermodysplasia verruciformis-like human papillomavirus types in malignant and premalignant skin

lesions of renal transplant recipients. Br J Dermatol 1994: 131: 226–230.

30. de Jong-Tieben L M, Berkhout R J, Smits H L et al. High frequency of detection of epidermodysplasia verruciformis-associated human papillomavirus DNA in biopsies from malignant and premalignant skin lesions from renal transplant recipients. J Invest Dermatol 1995: 105: 367–371.

31. Berkhout R J, Tieben L M, Smits H L et al. Nested PCR approach for detection and typing of epidermodysplasia verruciformis-associated human papillomavirus types in cutaneous cancers from renal transplant recipients. Detection of epidermodysplasia verruciformis-like human papillomavirus types in malignant and premalignant skin lesions of renal transplant recipients. J Clin Microbiol 1995: 33: 690–695.

32. Purdie K J, Pennington J, Proby C M et al. The promoter of a novel human papillomavirus (HPV77) associated with skin cancer displays UV responsiveness, which is mediated through a consensus p53 binding sequence. EMBO J 1999: 18: 5359–5369.

33. Jackson S, Storey A. E6 proteins from diverse cutaneous HPV types inhibit apoptosis in response to UV damage. Oncogene 2000: 19: 592–598.

34. Crish J F, Bone F, Balasubramanian S et al. Suprabasal expression of the human papillomavirus type 16 oncoproteins in mouse epidermis alters expression of cell cycle regulatory proteins. Carcinogenesis 2000: 21: 1031–1037.

35. Sedman S A, Barbosa M S, Vass W C et al. The full-length E6 protein of human papillomavirus type 16 has transforming and trans-activating activities and cooperates with E7 to immortalize keratinocytes in culture. J Virol 1991: 65: 4860–4866.

36. Pim D, Banks L. HPV-18 E6*I protein modulates the E6-directed degradation of p53 by binding to full-length HPV-18 E6. Oncogene 1999: 18: 7403–7408.

37. Kessis T D, Slebos R J, Nelson W G et al. Human papillomavirus 16 E6 expression disrupts the p53-mediated cellular response to DNA damage. Proc Natl Acad Sci USA 1993: 90: 3988–3992.

38. Funk J O, Waga S, Harry J B, Espling E, Stillman B, Galloway D A. Inhibition of CDK activity and PCNA-dependent DNA replication by p21 is blocked by interaction with the HPV-16 E7 oncoprotein. Genes Dev 1997: 11: 2090–2100.

39. Jones D L, Alani R M, Munger K. The human papillomavirus E7 oncoprotein can uncouple cellular differentiation and proliferation in human keratinocytes by abrogating p21Cip1-mediated inhibition of cdk2. Genes Dev 1997: 11: 2101–2111.

40. Peus D, Meves A, Vasa R A, Beyerle A, O'Brien T, Pittelkow M R. H2O2 is required for UVB-induced EGF receptor and downstream signaling pathway activation. Free Radic Biol Med 1999: 27: 1197–1202.

41. Ding M, Li J, Leonard S S et al. Differential role of hydrogen peroxide in UV-induced signal transduction. Mol Cell Biochem 2002: 234–235: 81–90.

42. Garmyn M, Degreef H. Suppression of UVB-induced c-fos and c-jun expression in human keratinocytes by N-acetylcysteine. J Photochem Photobiol B 1997: 37: 125–130.

43. Kulms D, Zeise E, Poppelmann B, Schwarz T. DNA damage, death receptor activation and reactive oxygen species contribute to ultraviolet radiation-induced apoptosis in an essential and independent way. Oncogene 2002: 21: 5844–5851.

44. Kulms D, Schwarz T. Independent contribution of three different pathways to ultraviolet-B-induced apoptosis. Biochem Pharmacol 2002: 64: 837–841.

45. Kuluncsics Z, Perdiz D, Brulay E, Muel B, Sage E. Wavelength dependence of ultraviolet-induced DNA damage distribution: involvement of direct or indirect mechanisms and possible artefacts. J Photochem Photobiol B 1999: 49: 71–80.

46. Romano G, Sgambato A, Mancini R et al. 8-hydroxy-2′-deoxyguanosine in cervical cells: correlation with grade of dysplasia and human papillomavirus infection. Carcinogenesis 2000: 21: 1143–1147.

47. Ford J M, Baron E L, Hanawalt P C. Human fibroblasts expressing the human papillomavirus E6 gene are deficient in global genomic nucleotide excision repair and sensitive to ultraviolet irradiation. Cancer Res 1998: 58: 599–603.

48. El-Mahdy M A, Hamada F M, Wani M A, Zhu Q, Wani A A. p53-degradation by HPV-16 E6 preferentially affects the removal of cyclobutane pyrimidine dimers from non-transcribed strand and sensitizes mammary epithelial cells to UV-irradiation. Mutat Res 2000: 459: 135–145.

49. Senkevich T G, Bugert J J, Sisler J R, Koonin E V, Darai G, Moss B. Genome sequence of a human tumorigenic poxvirus: prediction of specific host response-evasion genes. Science 1996: 273: 813–816.

50. Zhang W, Ramanathan C S, Nadimpalli R G, Bhat A A, Cox A G, Taylor E W. Selenium-dependent glutathione peroxidase modules encoded by RNA viruses. Biol Trace Elem Res 1999: 70: 97–116.

51. Shisler J L, Senkevich T G, Berry M J, Moss B. Ultraviolet-induced cell death blocked by a selenoprotein from a human dermatotropic poxvirus. Science 1998: 279: 102–105.

52. Gladyshev V N, Factor V M, Housseau F, Hatfield D L. Contrasting patterns of regulation of the antioxidant selenoproteins, thioredoxin reductase, and glutathione peroxidase, in cancer cells. Biochem Biophys Res Commun 1998: 251: 488–493.

53. Perquin M, Oster T, Maul A, Froment N, Untereiner M, Bagrel D. The glutathione-related detoxification system is increased in human breast cancer in correlation with clinical and histopathological features. J Cancer Res Clin Oncol 2001: 127: 368–374.

54. Lu Y P, Lou Y R, Yen P et al. Enhanced skin carcinogenesis in transgenic mice with high expression of glutathione peroxidase or both glutathione peroxidase and superoxide dismutase. Cancer Res 1997: 57: 1468–1474.